12-1997

BIOME-BGC simulations of stand hydrologic process for BOREAS

John S. Kimball
University of Montana - Missoula

Michael A. White

Steven W. Running
University of Montana - Missoula

Recommended Citation

Kimball, J. S., M. A. White, and S. W. Running (1997), BIOME-BGC simulations of stand hydrologic processes for BOREAS, J. Geophys. Res., 102(D24), 29043–29051, doi:10.1029/97JD02235

JOURNAL OF GEOPHYSICAL RESEARCH, VOL. 102, NO. D24, PAGES 29,043–29,051, DECEMBER 26, 1997

BIOME-BGC simulations of stand hydrologic processes for BOREAS

John S. Kimball, Michael A. White, and Steve W. Running
Numerical Terradynamic Simulation Group, School of Forestry, University of Montana, Missoula

Abstract. BIOME-BGC is a general ecosystem model designed to simulate hydrologic and biogeochemical processes across multiple scales. The objectives of this investigation were to compare BIOME-BGC estimates of hydrologic processes with observed data for different boreal forest stands and investigate factors that control simulated water fluxes. Model results explained 62 and 98% of the respective variances in observed daily evapotranspiration and soil water; simulations of the onset of spring thaw and the dates of snowpack disappearance and accumulation also generally tracked observations. Differences between observed and simulated evapotranspiration were attributed to model assumptions of constant, growing season, overstory leaf areas that did not account for phenological changes and understory effects on stand daily water fluxes. Vapor pressure deficit and solar radiation accounted for 58–74% of the variances in simulated daily evapotranspiration during the growing season, though low air temperature and photosynthetic light levels were found to be the major limiting factors regulating simulated canopy conductances to water vapor. Humidity and soil moisture were generally not low enough to induce physiological water stress in black spruce stands, though low soil water potentials resulted in approximate 34% reductions in simulated mean daily canopy conductances for aspen and jack pine stands. The sensitivity of evapotranspiration simulations to leaf area (LAI) was less than expected because of opposing responses of transpiration and evaporation to LAI. The results of this investigation identify several components within boreal forest stands that are sensitive to climate change.

1. Introduction

The boreal forest covers a broad circumpolar band across the Eurasian and North American continents and represents approximately 11% of the Earth's total land area [*Bonan and Shugart*, 1989]. Global climate simulation studies indicate that the boreal forest region will experience significant warming and drying in response to increases in atmospheric CO_2 and other greenhouse gases [*Monserud et al.*, 1993; *Houghton et al.*, 1990; *Manabe and Stouffer*, 1980]. This is of major concern, since the boreal forest region is thought to contain 16–24% of the world's soil carbon [*Gates*, 1993]. Significant warming in this region may result in fairly rapid, large-scale displacement and redistribution of boreal forests as well as enhanced release of CO_2 to the atmosphere [*Neilson and Marks*, 1994; *Pastor and Post*, 1988; *Emanuel et al.*, 1985]. These factors may result in an intensification of global warming.

The Boreal Ecosystem-Atmosphere Study (BOREAS) is an international study designed to assess the interactions between the boreal forest biome and the atmosphere. A primary objective of this project is to evaluate possible feedbacks between the boreal forest, global water, and biogeochemical cycles due to global warming [*BOREAS Science Steering Committee*, 1991]. A critical goal of this project is to integrate point measurements across multiple spatial and temporal scales using process-level models of the boreal forest water, energy, and biogeochemical cycles. BIOME-BGC is a general ecosystem process model designed to simulate hydrologic and biogeochemical processes across multiple scales [*Running and Hunt*, 1993]. Our goals are to utilize BIOME-BGC logic to (1) synthesize and establish linkages between measured data at various spatial and temporal scales and (2) quantify key processes regulating water fluxes. More specifically, we compare BIOME-BGC simulations of hydrologic processes for different boreal forest stands with daily evapotranspiration and soil water and snow depth measurements and investigate climate and stand characteristics that control simulated water fluxes.

2. Experimental Design

2.1. BIOME-BGC

BIOME-BGC (biogeochemical cycles) simulates hydrologic and biogeochemical processes across multiple biomes based on the logic that differences in process rates between biomes are primarily a function of climate and general life-form characteristics. BIOME-BGC is similar in scope and logic to the FOREST-BGC model described by *Running and Coughlan* [1988], except that site and vegetation components have been determined and tested for multiple biomes, including coniferous and deciduous forests, grassland, shrubland, and alpine cover types [*Kremer and Running*, 1996; *Running and Hunt*, 1993]. The boreal forest represents a unique environment characterized by flat terrain and a short growing season. Measurements from other BOREAS investigators have shown large sensible heat fluxes during the growing season resulting from low evapotranspiration rates and low solar albedos for coniferous stands [*Sellers et al.*, 1995]. This investigation constitutes our initial effort to test and improve BIOME-BGC logic at the stand level in order to improve model representation of the boreal forest biome in regional applications.

Paper number 97JD02235.
0148-0227/97/97JD-02235$09.00

The water balance portion of BIOME-BGC utilizes daily meteorological data in conjunction with general stand and soil information to predict evaporation, transpiration, soil moisture, snow water equivalent depth, and soil outflow of water at a daily time step. BIOME-BGC is general in the sense that the surface is represented by singular, homogeneous canopy, snow, and soil layers.

Precipitation is categorized as rain or snow using a prescribed air temperature threshold of 0.0°C. Rainfall is intercepted by the canopy using a prescribed interception coefficient based on leaf area index (LAI). Intercepted precipitation is then evaporated from the canopy using a Penman combination method with a prescribed boundary layer conductance [*Running and Coughlan*, 1988].

All remaining rainfall is routed directly to the surface. Snowfall is not intercepted by the vegetation canopy and is passed directly to the surface. Snowfall is stored as depth of water equivalent, and no attempt is made to account for snowpack depth or density. If the mean daily air temperature is less than 0.0°C, snowpack sublimation is estimated according to the amount of daily net solar radiation ($R_{n,s}$) at the surface. If the air temperature is greater than 0.0°C, snowmelt is calculated using a degree-day method and $R_{n,s}$.

Transpiration l_T is regulated by the canopy conductance to water g_c and daily meteorological conditions including air temperature, vapor pressure deficit (VPD) and $R_{n,s}$. The maximum canopy conductance to water $g_{c,\max}$ defines the upper boundary of the transpiration rate and is determined by LAI and prescribed leaf-scale boundary layer, cuticular and maximum stomatal conductances; g_c is reduced when air temperatures, VPDs, photosynthetic photon flux densities (PPFD), or soil water potentials (PSI) deviate from prescribed optimal conditions [*Leuning*, 1990; *Running and Coughlan*, 1988; *Jarvis and Morison*, 1981]. BIOME-BGC represents the canopy as a "big leaf," in that all units of leaf area in the canopy are represented using a single, canopy-averaged conductance. This assumption is generally not valid at subdaily (e.g., hourly) time steps, since the reduction of irradiance at lower vertical layers of the canopy reduces conductances at the bottom of the canopy. The big leaf assumption is strengthened, however, by the integrative effects of a daily time step and by the implicit assumption that the allocation of leaf nitrogen between light harvesting and carbon fixing enzymes over depth in the canopy varies in response to the canopy light environment, allowing an optimized use of intercepted radiation [*Evans*, 1989].

Soil evaporation is computed using a Penman-Monteith combination approach with prescribed boundary layer and soil conductances [*Running and Coughlan*, 1988]. Soil conductances are decreased using an inverse, linear exponential function based on the number of days since a rainfall event [*Hanks*, 1985]. The soil layer is represented as a simple bucket in which no movement of soil water between adjacent soil layers occurs, and soil storage is defined by a prescribed soil depth and field capacity. Rainfall and snowmelt are passed to the soil layer until the soil is at field capacity, whereby all excess water is passed to outflow. Water is removed from the soil layer by surface evaporation and transpiration. PSI is calculated from soil water content and prescribed soil texture, *b* parameter and soil depth information following *Saxton et al.* [1986] and *Cosby et al.* [1984].

BIOME-BGC uses daily maximum and minimum air temperatures, humidity, incident solar radiation, and precipitation to determine daily hydrologic characteristics. Incident shortwave radiation is simulated using MT-CLIM logic described by *Running et al.* [1987]. The estimated total daily incident radiation is attenuated through the vegetation canopy using Beer's formulation and a prescribed extinction coefficient modulated by LAI. $R_{n,s}$ is estimated using prescribed albedos for snow and vegetated surfaces. Maximum and minimum daily air temperatures are used to estimate mean daily air temperatures. Minimum daily air temperature is assumed equal to the dew point and is used with mean daily air temperature to estimate VPD. $R_{n,s}$ and VPD are used with estimated conductances in the Penman and Penman-Monteith equations to derive mean daily latent energy fluxes. These results are combined with estimated day length information to derive daily l_T, evaporation l_E, and evapotranspiration l_{ET}.

2.2. Study Sites

The BOREAS study region consists of a 1 × 10^6 km^2 area covering portions of central Saskatchewan and Manitoba [*Sellers et al.*, 1995]. Within this region are two intensive study sites, each approximately 10,000 km^2 in area. The southern study area (SSA) is located near Prince Albert, Saskatchewan (53.2°N, 105.7°W), whereas the northern study area (NSA) is located roughly 500 km to the northwest near Thompson, Manitoba (55.7°N, 97.8°W). The BOREAS study region consists of relatively flat to gently rolling terrain with mean elevations from 261 m in the NSA to 520 m in the SSA. Vegetation cover is predominantly coniferous with low species diversity and productivity relative to temperate forests. Understory vegetation is generally composed of sparse shrubs with extensive moss and lichen ground cover. Temperature and solar radiation play a major role in controlling boreal forest productivity by limiting energy, water supply, and nutrient availability to plants for much of the year. The growing season is generally restricted to only a few months between May and September when daily air temperatures rise above 0.0°C.

Eddy flux and soil moisture measurement networks were established within selected forest stands considered representative of the boreal forest region [*Sellers et al.*, 1995]. Tower eddy flux measurements of water fluxes above the forest overstories and soil moisture measurements were obtained over three intensive field campaigns (IFCs) during the 1994 growing season. Detailed descriptions of site characteristics and data collection are presented by *Sellers et al.* [1995], *Black et al.* [1996], *Haddeland and Lettenmaier* [1995], and *Baldocchi et al.* [1997]. Daily evapotranspiration, soil moisture, and snow water equivalent were simulated for five flux tower sites within the NSA and SSA and compared with measured results. Two sites were examined within the NSA representing young jack pine (NYJP) and old black spruce (NOBS) forest types. Three sites were also examined within the SSA consisting of old black spruce (SOBS), old jack pine (SOJP), and old aspen (SOAS) forest types.

The jack pine sites were 30–80% forest covered, with jack pine (*Pinus banksiana* Lamb.) ranging in ages from less than 15 years at the NYJP site to between 70 and 90 years at the SOJP site. Canopy heights ranged from 12–15 m at the SOJP site to 4–5 m at the NYJP site. Understory vegetation was sparse, consisting predominantly of isolated groups of alder (*Alnus crispa* (Ait.) Pursh) with an extensive surface cover of lichens (*Cladina* spp.), bearberry (*Arctostaphylos uva-ursi*), and bog cranberry (*Vaccinium vitisideae*). Soils were coarse textured, sandy, and well drained and were classified as a degraded Eutric Brunisol/Orthic Eutric Brunisol.

Table 1. BIOME-BGC Physiological and Soil Parameters for BOREAS Study Sites

	NOBS	NYJP	SOBS	SOJP	SOAS
LAI (one-sided)	4.51	1.68	3.84	2.40	2.70
Minimum leaf conductance, mm/s	0.01	0.01	0.01	0.01	0.05
Maximum leaf stomatal conductance, mm/s	1.0	1.0	1.0	1.0	5.0
Maximum leaf boundary layer conductance, mm/s	0.8	0.8	0.8	0.8	0.8
Optimal temperature for g_c, °C	15.0	15.0	15.0	15.0	15.0
Maximum temperature for g_c, °C	40.0	40.0	40.0	40.0	40.0
PSI at start of g_c reduction, MPa	− 0.5	− 0.5	− 0.5	− 0.5	− 0.5
PSI at complete g_c reduction, MPa	− 1.7	− 2.0	− 1.7	− 1.7	− 2.3
VPD at start of g_c reduction, kPa	1.0	1.0	1.0	1.0	1.0
VPD at complete g_c reduction, kPa	4.0	4.0	4.0	4.0	4.0
Effective soil depth, m	0.5	0.5		0.5	0.5
Volumetric soil water capacity, %	48	40	48	40	48
Soil field capacity, %	44	10	40	11	34
Available soil water, mm	220	50	200	57	170
Soil b parameter	10.39	2.79	10.39	2.79	10.39
Site short-wave albedo (snow-free conditions)	0.10	0.10	0.10	0.10	0.20

LAI, leaf area index; PSI, soil water potentials; VPD, vapor pressure deficit; NOBS, old black spruce in northern study area (NSA); NYJP, young jack pine in NSA; SOBS, old black spruce in southern study area (SSA); SOJP, old jack pine in SSA; SOAS, old aspen in SSA.

The SOBS and NOBS sites were 30–70% forest covered with mature stands of black spruce (*Picea mariana*) from 60 to 80 years in age with tree heights ranging from 7 to 18 m. Soils consisted of poorly drained silt and clay overlain by a thick moss layer (*Sphagnum* spp., *Pleurozium* spp.).

The SOAS site was 30–60% forest covered with an extensive stand of mature aspen (*Populus tremuloides*), approximately 70 years old, with average tree heights of approximately 21 m. The aspen understory was extensive and was mainly composed of hazelnut (*Corylus cornuta* Marsh.), approximately 2 m in height, interspersed with alder (*Alnus crispa* (Ait.) Pursch). Soils consisted of Orthic Gray Luvisol with a medium to moderately fine silty clay texture.

2.3. Measurement Data

Air temperature and precipitation were measured at approximate 15 min intervals at each of the study sites during 1994. These data were obtained from BOREAS principal investigators at each study site and the Saskatchewan Research Council's Automatic Meteorological Stations (AMS) mesonet database. Detailed descriptions of the methods and instruments used to obtain these data are provided by *Sellers et al.* [1995], *Baldocchi and Vogel* [1996], and *Black et al.* [1996]. The 1994, 15 min data records for each study site were incomplete because of periods of instrument malfunction and calibration and measurement inactivity. Continuous data records for 1994 were obtained for each study site by temporally interpolating missing data or substituting data from adjacent sites. Daily maximum and minimum air temperatures, precipitation, and solar radiation were then derived from the continuous 15 min data records for each site.

BIOME-BGC simulations of daily evapotranspiration, soil water, and snow water equivalent were compared with canopy water flux, soil water, and snow depth measurements collected over selected periods during 1994. Latent energy fluxes were measured above the forest canopy using an eddy covariance flux method. These data were obtained from the principal investigators at each site [*Sellers et al.*, 1995]. Detailed descriptions of flux measurement methods and instrumentation are given by *Baldocchi and Vogel* [1996] and *Black et al.* [1996]. Latent energy flux measurements were converted to mass fluxes, integrated over 24 hour time periods and compared with simulated results.

Volumetric soil water data were collected at each study site over selected days during 1994 by a team led by Richard Cuenca from Oregon State University. Soil water data were measured at the NOBS, SOAS, and SOBS sites using time domain reflectometry (TDR) equipment, while a neutron probe was used at the NYJP and SOJP sites. Soil water was monitored at each study site from three to six sample locations spaced 25–120 m from the flux towers. Measurements were taken from the surface to 120 cm soil depths at approximate 10 cm intervals. Daily measurements were integrated over 0.5 m soil depths, and all sample locations were averaged at each study site and compared with simulated results. Simulated and observed daily soil water levels were evaluated at most sites except the NOBS site, where changes in daily soil moisture were compared. TDR soil water measurements were found to be unreliable at this site because of high organic matter and soil water levels; however, measured changes in daily soil water levels provided measures of accuracy of approximately ±2% [*Cuenca et al.*, this issue].

Snow depth information was obtained for 1994 at the SOAS and SOJP sites from the Saskatchewan Research Council's AMS mesonet database. Snow depth was measured using an ultrasonic snow depth gage situated beneath the canopy. The instrument had a measurement range of 0.6–10 m, with an estimated measurement accuracy of approximately ±1 cm. Snow depth measurements were used to gage the accuracy of model simulations of the timing of the spring thaw and the dates of snowpack disappearance and accumulation.

2.4. Model Initialization

BIOME-BGC requires general information about plant and soil characteristics in order to monitor the daily water balance at a site. A list of critical parameters used to define soil and stand characteristics at the five study sites is presented in Table 1. These parameters were obtained from both published literature for these genera and unpublished site observations from BOREAS researchers. When data were not available for these genera, parameters were obtained from related genera under similar environmental conditions.

Table 2. The 1994 Daily Meteorological Data Summary for BOREAS Sites

	NSA	SSA
Growing season, days	151	178
Average growing season day length, hours	14.6	14.
Annual precipitation, mm	447	421
Growing season precipitation, mm	250	356
Annual air temperature, °C		
Average	−1.6	−1.0
Standard deviation	16.0	14.8
Growing season air temperature, °C		
Average	11.8	11.6
Standard deviation	6.1	6.3
Growing season VPD, kPa		
Average	0.61	0.59
Standard deviation	0.31	0.29
Growing season solar radiation, W/m^2		
Average	298	276
Standard deviation	121	120

NSA, northern study area; SSA, southern study area.

The effective soil depth defines the vegetation rooting depth and is used with soil texture information to determine the maximum amount of soil water available for evapotranspiration. The effective soil depth was set at 0.5 m following *Haddeland and Lettenmaier* [1995] and *Sellers et al.* [1995]. Soil volumetric water capacity, field capacity, and *b* parameter values were derived from measurements collected at the study sites during 1994 by *Cuenca et al.* [this issue] and values reported in the literature for representative soil types [*Cosby et al.*, 1984; *Hillel*, 1980].

Mean daily vegetation solar albedos for snow-free conditions were estimated from site observations reported by *Sellers et al.* [1995], whereas the mean daily solar albedo for snow was set at 0.8 [*Brutsaert*, 1988]. Canopy extinction of solar radiation was set at −0.5 based on data for temperate deciduous and evergreen forests [*Hunt and Running*, 1992; *Jarvis and Leverenz*, 1984].

Estimates of mean annual LAI were derived from optical leaf area measurements of canopy overstories conducted over approximately three periods during the 1994 growing season by *Chen* [1996]. No attempt was made to configure the model to represent understory canopy contributions to daily water fluxes or seasonal changes in LAI. Leaf cuticular, boundary layer, and maximum stomatal conductances were obtained from *Nobel* [1991] and *Waring and Schlesinger* [1985]. A wide range of values has been reported in the literature for these conductances. Values used for this investigation represent the lower end of this range based on observations that reduced nutrient availability in boreal regions result in reduced rates of carbon uptake and lower stomatal conductances [*Baldocchi and Vogel*, 1996; *Shulze et al.*, 1994]. Temperature, VPD, and PSI bounds on g_c were estimated from values reported in the literature for coniferous and deciduous cover types [*Baldocchi and Vogel*, 1996; *Waring and Schlesinger*, 1985; *Waring and Franklin*, 1979; *Vowinckel et al.*, 1975].

BIOME-BGC was run over a 2 year period for each study site. The model was initialized using 1989 AMS mesonet station data from the Thompson airport (55.8°N, 97.9°W) for study sites in the NSA, and Prince Albert airport (53.2°N, 105.7°W) and Waskesiu Lake (53.9°N, 106.1°W) for study sites in the SSA. All analyses of model results were done for the second year using the 1994 meteorological database described above.

3. Results and Discussion

3.1. Meteorological Characteristics

The 1994 daily meteorological data records for the study sites are summarized in Table 2. The NSA was slightly colder than the south, with a mean annual air temperature of −1.6°C, compared with 1.0°C within the SSA. The active physiological, or growing, season was defined as the number of days with minimum daily air temperatures above 0.0°C. The growing season ranged over an approximate 151 day period within the NSA and was approximately 1 month longer in the SSA. The average day length during the growing season in the SSA was 14.1 hours, while the day length in the NSA was approximately 30 min longer because of its more northerly location. Daily incident solar radiation during the growing season averaged 276 and 298 W m^{-2} for sites in the NSA and SSA, respectively. Mean daily air temperatures during the growing season were similar between the NSA and SSA, averaging 11.7°C. Mean daily VPDs for the same period averaged 0.59 kPa in the SSA and 0.61 kPa in the NSA. Overall, 1994 meteorological records for the study sites show that air temperature, humidity, and solar radiation were generally similar between the NSA and SSA during the growing season.

Annual precipitation for 1994 averaged 447 and 421 mm for sites in the NSA and SSA, respectively. The greater amount of annual precipitation in the NSA was due to greater winter snowfall relative to the SSA. However, the SSA received approximately 360 mm of rainfall during the growing season, which was approximately 100 mm greater than the NSA received.

3.2. Model Comparisons With Measured Results

Model simulations of daily evapotranspiration were compared with daily water fluxes derived from stand eddy flux measurements collected during the 1994 growing season. Five-day means of predicted and observed l_{ET} are presented in Figure 1 for selected stands. Positive fluxes represent transfer away from the surface, whereas negative values denote the reverse. The lengths of the sample periods for measured data varied from 15 (NYJP) to 230 (SOAS) days and averaged only 93 (standard deviation (s.d.) = 72) day for all sites. Sample periods were limited by sensor malfunctions and the high cost and difficulty associated with maintaining continuous measurements over longer periods. Measurement uncertainties were estimated to be of the order of ±15% [*Baldocchi and Vogel*, 1996].

Mean daily differences between simulated and observed l_{ET} ranged from 0.0 mm d^{-1} at the NOBS site to 0.3 mm d^{-1} at the SOBS site, whereas l_{ET} differences averaged 0.2 (s.d. = 0.6) mm d^{-1} for all sites (Table 3). Root mean squared errors (RMSE) between observed and simulated l_{ET} ranged from 0.2 (NYJP) to 0.7 (SOBS) mm d^{-1} and averaged 0.5 (s.d. = 0.2) mm d^{-1} for all sites. These RMSE values constituted 18% (NYJP) to 50% (SOAS) of the mean measured l_{ET} at each site, averaging approximately 34% for all sites.

Simulated l_{ET} explained 62.3% (s.d. = 0.6 mm d^{-1}) of the variance in observed l_{ET} for all sites (Figure 2). Simulated results also tended to underestimate observations by approximately 9.7%. Differences between simulated and observed results were mainly attributed to model generalizations of stand morphology. Leaf area was represented in the model using a constant, seasonal average LAI based on overstory measurements conducted at the beginning, middle, and end of the growing season at each study site. LAI measurements, however, showed approximate seasonal variations of 12, 18, and 34% of mean values for black spruce, jack pine, and aspen stands, respectively. These effects were more pronounced at the SOAS site (Figure 1), where simulations tended to overestimate observed l_{ET} at the beginning of the growing season and underestimate observations in the middle of the growing season, when leaf area was generally greatest. Understory contributions to l_{ET} were also not represented in model simulations because only overstory LAI information was used to characterize stand leaf areas. Observations by *Black et al.* [1996], however, indicate that l_{ET} from the hazelnut understory constituted a significant proportion of seasonal fluxes at the SOAS site.

Table 3. Summary of Simulated and Measured 1994 Evapotranspiration and Soil Water for BOREAS Study Sites

	Evapotranspiration				
Site	BIOME-BGC Average, mm/d	Measured Average, mm/d	Estimated Measured Uncertainty, %	RMSE, mm/d	Sample Period, days
SOJP	1.4	1.3	±15	0.5	71
SOBS	1.8	2.1	±15	0.7	76
SOAS	0.9	1.0	±15	0.5	230
NOBS	1.4	1.4	±15	0.4	75
NYJP	1.0	1.1	±15	0.2	15

	Soil Water				
	BIOME-BGC Average, %	Measured Average, %	Measured Variation, %	RMSE, %	Sample Period, days
SOJP	7.9	8.4	±0.5	1.6	35
SOBS	35.3	33.7	±3.3	2.7	26
SOAS	29.5	29.1	±3.2	1.4	33
NOBS*	−0.1	−0.1	±2.9	3.6	12
NYJP	6.8	6.7	±0.7	1.0	32

RMSE, root mean squared error. See Table 1 footnote for definition of sites.

* Sites where the change in soil water is given.

Daily soil water simulations were compared with neutron probe and TDR measurements collected during the 1994 growing season. Five-day means of simulated and observed daily soil water are plotted in Figure 3 for selected stands. Soil water measurements generally showed high spatial variability at each site, with differences from 0.5 to 3.3% between sample locations (Table 3). Measurement uncertainties were also approximately ±2%. Daily differences between simulated and observed soil water averaged approximately 0.5% for all sites. RMSE values between observed and simulated soil water ranged from 1.0% (NYJP) to 3.6% (NOBS). Simulated daily soil water explained 97.7% of the variance in measured results for all sites with an estimation error of 1.9% (Figure 4). Overall, simulated and measured results were generally consistent, given the ranges of measurement uncertainty due to instrument accuracy and site soil water variation.

Model simulations of depths of snow water equivalent were compared with snowpack depth measurements to evaluate whether simulations of the periods of spring thaw, and snowpack accumulation and disappearance were reasonably accurate. Simulated and observed results for the SOAS and SOJP sites are plotted in Figure 5. The predicted general onset of spring thaw (i.e., point where Δ snowpack becomes predominantly negative) occurred on February 24 and 26 at the SOJP and SOAS sites. Simulated dates of snowpack disappearance

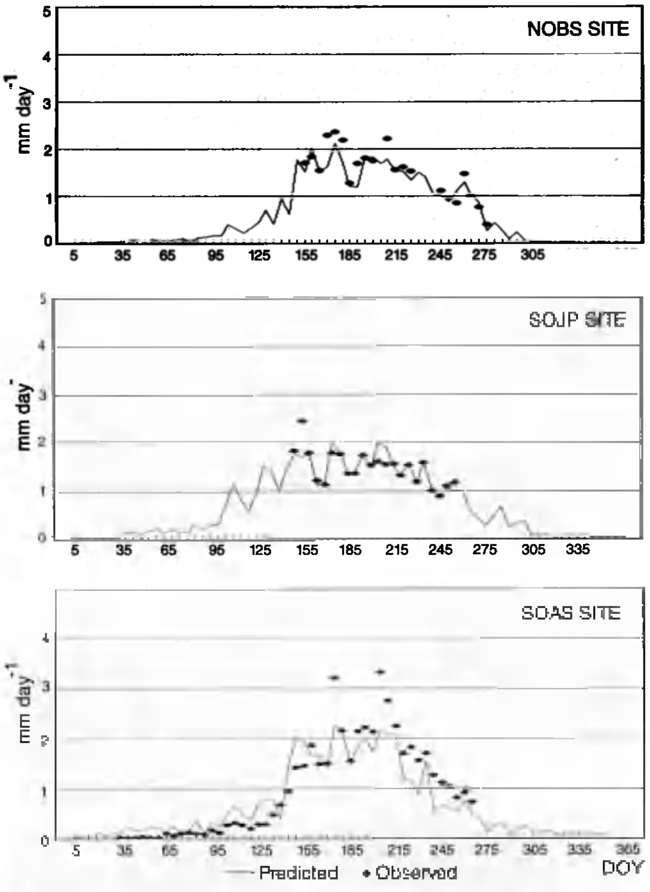

Figure 1. Plotted 5-day means of simulated and observed 1994 daily evapotranspiration for NOBS, SOJP, and SOAS study sites.

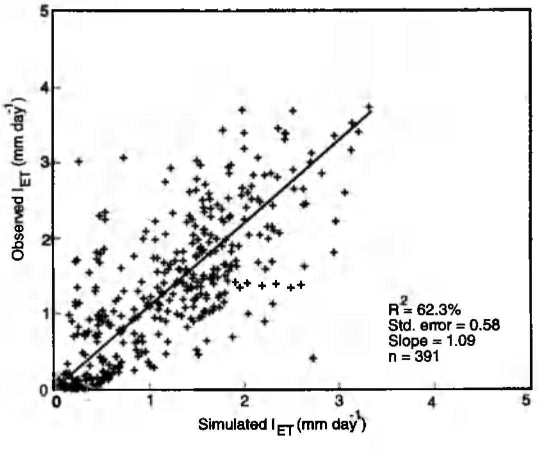

Figure 2. Linear regression results between simulated and observed 1994 daily evapotranspiration for all sites.

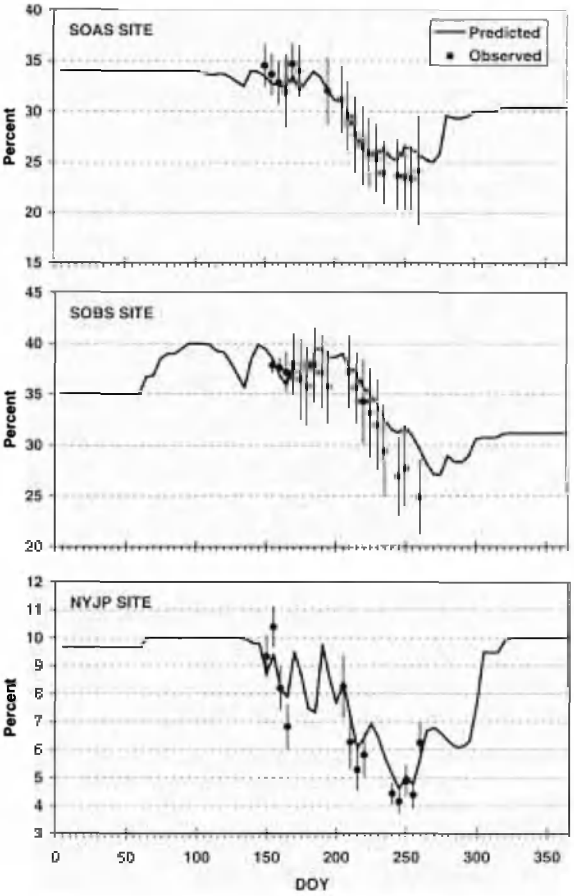

Figure 3. Plotted 5-day means of simulated and mean observed 1994 daily volumetric soil moisture over a 0.5 m soil depth for the NYJP, SOBS, and SOAS study sites; the vertical lines show the standard deviation of the observations at each site.

occurred on April 16 and 17 for the SOAS and SOJP sites, respectively. Simulated dates of snowpack accumulation at the end of the growing season occurred on November 1 for the SOAS and SOJP sites. Model results were generally within 14 days of observed snowpack disappearance dates and within 2 days of observed snowpack appearance and onset of spring thaw dates for the two sites where snowpack depth measurements were taken.

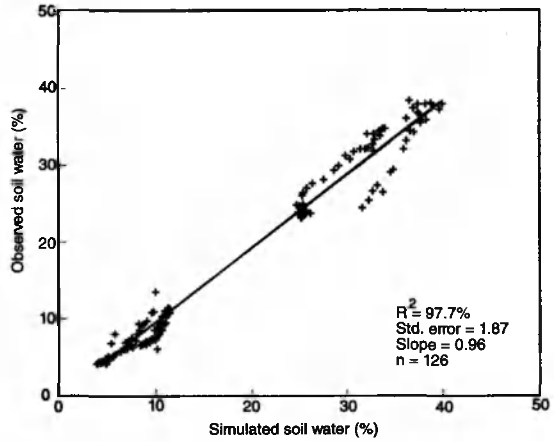

Figure 4. Linear regression results between simulated and observed 1994 daily soil moisture for all sites.

3.3. Controls on Simulated Water Fluxes

BIOME-BGC simulations of transpiration and evaporation components of daily l_{ET} were used to evaluate physical and climate controls on estimated water fluxes. These results are based on our present understanding of boreal stands using information currently available and have not been validated by direct measurements. During the 1994 growing season, simulated l_{ET} averaged 1.1 mm d^{-1} at all sites (Table 4). Annual evapotranspiration ($l_{\mathrm{ET,ann}}$) for 1994 ranged from 197 mm (NYJP) to 271 mm (SOBS) and represented approximately 56% of annual precipitation ($l_{P,\mathrm{ann}}$). Annual transpiration ($l_{T,\mathrm{ann}}$) represented less than half of $l_{\mathrm{ET,ann}}$ except at the black spruce stands, where $l_{T,\mathrm{ann}}$ constituted approximately 63% of $l_{\mathrm{ET,ann}}$. Transpiration represented greater proportions of $l_{\mathrm{ET,ann}}$ at these sites because black spruce LAI values were larger than the other stands, resulting in enhanced l_T. Increased leaf area also reduced surface l_E and sublimation due to greater canopy extinction of solar radiation and reduced surface $R_{n,s}$.

The magnitudes of l_{ET} simulations within each stand were largely determined by the magnitudes of VPD, $R_{n,s}$, and canopy conductances to water vapor. Individually, VPD and $R_{n,s}$ explained 75% and 44% of the variance in l_{ET}, respectively, for sites in the NSA. In the SSA, VPD and $R_{n,s}$ each accounted for approximately 37% of the variance in l_{ET}. Together, VPD and $R_{n,s}$ explained approximately 78% (NSA) and 51% (SSA) of the variance in l_{ET}.

The canopy water vapor conductance term in BIOME-BGC (g_c) defines the bulk physiological control of vegetation to water vapor loss through transpiration. During the 1994 grow-

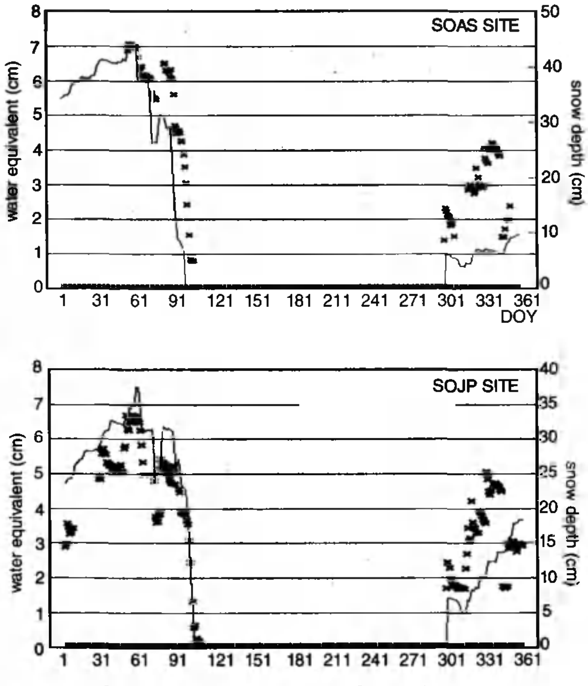

Figure 5. Plotted 1994 simulated daily depth of snow water equivalent and observed snowpack depth for SOAS and SOJP sites.

Table 4. Summary of 1994 Simulated Water Fluxes for BOREAS Study Sites

Site	Growing Season Average l_{ET}, mm/d	Standard Deviation, mm/d	$l_{\mathrm{ET,ann}}$, mm	$l_{T,\mathrm{ann}}/l_{\mathrm{ET,ann}}$, %	$l_{\mathrm{ET,ann}}/l_l$, %
SOJP	1.15	0.59	236	44	57
SOBS	1.40	0.62	271	60	69
SOAS	1.10	0.77	226	39	53
NOBS	1.13	0.67	260	65	59
NYJP	0.94	0.54	197	34	44

See Table 1 footnote for definition of sites; l_{ET}, evapotranspiration; $l_{\mathrm{ET,ann}}$, annual evapotranspiration; $_{T,\mathrm{ann}}$, annual transpiration; $l_{P,\mathrm{ann}}$, annual precipitation.

ing season, g_c averaged 68% (s.d. = 3.8) and 66% (s.d. = 8.2) of $g_{c,\max}$ for sites in the NSA and SSA, respectively. Air temperature and PPFD were the primary factors influencing g_c in the NSA and were responsible for approximately 62 and 38% of the reduction in g_c, respectively. In the SSA, air temperature was responsible for 47–70% of the reduction in g_c at the SOJP and SOBS sites, while PPFD was responsible for 27–50% of the g_c reduction. Temperature and PPFD generally showed the greatest effect on g_c during the beginning and end of the growing season, when low solar radiation and air temperature conditions were predominant.

Simulated PSI levels generally remained high (> −0.5 MPa) throughout the year at most sites except the SOAS and SOJP sites, which had relatively sandy soils. Low PSI levels (< −0.5 MPa) occurred over an 80 day period at the SOAS site beginning the first week of August and continuing through September. This period generally coincided with the observed onset of aspen and hazelnut canopy senescence [*Black et al.*, 1996]. Simulated daily PSI during this period averaged −1.7 MPa over the prescribed 0.5 m soil depth and was responsible for approximately 75% of the reduction in g_c, which averaged 52% of $g_{c,\max}$. Simulated daily PSI also averaged −1.1 MPa at the SOJP site over a 27 day period beginning the last week of August. Low PSI values during this period contributed to 19% of the reduction in g_c, which averaged 67% of $g_{c,\max}$.

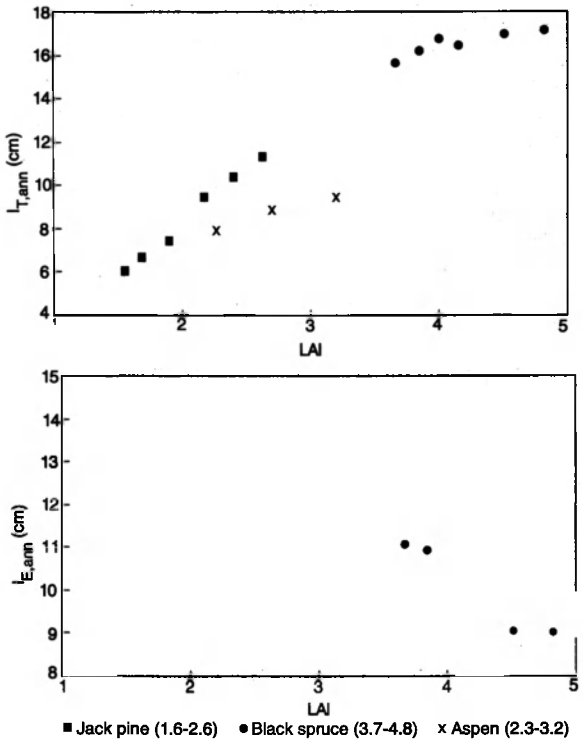

Figure 6. Scatterplots of simulated annual transpiration and evaporation against observed LAI values for all sites; annual fluxes were derived from BIOME-BGC using mean LAI values measured within three consecutive periods at each study site during the 1994 growing season.

The canopy conductance to water vapor was restricted when the VPD exceeded 1.0 kPa, reducing l_T accordingly. Complete g_c reduction occurred when the VPD approached 4.0 kPa. Mean daily vapor pressure deficits exceeded 1.0 kPa for approximately 23 days in the NSA and from 5 (SOAS) to 30 (SOJP) days in the SSA over the 1994 growing season. Daily VPDs during these periods in both regions averaged 1.1 kPa, with maximum daily values approaching 1.4 kPa; g_c was only marginally affected under these conditions, and VPD was never responsible for more than 20% of the reduction in g_c.

Stand differences in the relative proportions of simulated $l_{\mathrm{ET,ann}}$ represented by $l_{T,\mathrm{ann}}$ and $l_{E,\mathrm{ann}}$ within the SSA and NSA were attributed primarily to physiological variables such as LAI, since meteorological conditions were fairly consistent between sites. A scatterplot of simulated $l_{T,\mathrm{ann}}$ with corresponding ranges of measured LAI for all stands implies a positive relationship between transpiration and leaf area (Figure 6). Increasing LAI from 3.7 to 4.8 resulted in a 10% (1.6 cm) increase in $l_{T,\mathrm{ann}}$ for black spruce. Similar increases across the ranges of measured LAI for aspen and jack pine stands resulted in respective increases of 19% (1.5 cm) and 86% (5.2 cm) in $l_{T,\mathrm{ann}}$. Simulated $l_{E,\mathrm{ann}}$ shows a contrasting, inverse relationship with leaf area. Increases across the ranges of measured LAI resulted in 19% (2.1 cm), 9% (1.3 cm), and 7% (0.9 cm) reductions in $l_{E,\mathrm{ann}}$ for black spruce, jack pine, and aspen stands, respectively. This relationship is due to a reduction in $R_{n,s}$ at the surface with increasing leaf area, resulting in reduced snowpack sublimation and surface evaporation. The net effect of LAI on $l_{\mathrm{ET,ann}}$ is lower than might be expected because of the contrasting relationship between evaporation and transpiration.

4. Summary and Conclusions

Comparisons between BIOME-BGC simulations and observed results were encouraging, given the general nature of model parameterization of stand morphology. Model results corresponded well with available soil water and snow depth measurements, whereas daily differences between observed and simulated evapotranspiration were often large. These differences were attributed to model assumptions of constant, overstory LAI values during the growing season that did not account for phenological changes in leaf area and understory effects on stand evapotranspiration. Simulations of stand fluxes are likely to improve, however, as more information is gained regarding stand phenological changes and understory processes from BOREAS field campaigns.

Vapor pressure deficit and solar radiation accounted for more than half of the variance in simulated daily evapotranspiration rates during the growing season, though low air temperature and photosynthetic light levels were major factors limiting simulated canopy conductances to water vapor. Humidity and soil moisture were generally not low enough to induce physiological water stress in black spruce stands, though low soil water potentials resulted in moderate reductions in simulated canopy conductances for aspen and jack pine stands near the end of the growing season, corresponding to the observed onset of canopy senescence at the aspen site. The sensitivity of evapotranspiration simulations to leaf area was less than expected because of opposing responses of transpiration and evaporation to LAI.

This investigation identifies several components within boreal forest stands that appear to be sensitive to climate change, though the nature of various feedbacks and the total response of the system require further investigation. Warmer air temperatures and longer growing seasons may enhance evapotranspiration rates, though lower humidities and reduced soil water levels could minimize evapotranspiration by inducing water stress. Lower evapotranspiration rates may only serve to enhance warmer temperatures and drier conditions on a regional scale, inducing further moisture stress. Adjustments in LAI through logging and fire may have only minimal impact on annual evapotranspiration. The southern portion of the boreal forest currently appears more sensitive to warmer, drier conditions than more northerly regions because of the longer growing season. Sites in upland areas with sandy soils may be particularly susceptible to water stress because of the reduced soil water holding capacities of these areas.

Acknowledgments. This study was funded under grants NAG-52297 and NAGW-4234. Much of the meteorological data used in this investigation were provided by the Saskatchewan Research Council's AMS mesonet database. We wish to thank the BOREAS project and the following BOREAS teams for providing the soil, eddy flux, LAI, and additional meteorological and stand physiological data that made this paper possible: AFM-7, HYD-1, RSS-7, TE-6, TE-9, TF-1, TF-3, TF-5, TF-7, TF-8, TF-9, TF-10, TF-11, TGB-3, and TGB-12.

References

Baldocchi, D. D., and C. A. Vogel, Energy and CO_2 flux densities above and below a temperate broad-leaved forest and a boreal pine forest, *Tree Physiol.*, *16*, 5–16, 1996.

Baldocchi, D. D., C. A. Vogel, and B. Hall, Seasonal variation of carbon dioxide exchange rates above and below a boreal jack pine forest, *Agric. For. Meteorol.*, *83*, 147–170, 1997.

Black, T. A., G. den Hartog, H. H. Neumann, P. D. Blanken, P. C. Yang, C. Russell, Z. Nesic, X. Lee, S. G. Chen, and R. Staebler, Annual cycles of water vapour and carbon dioxide fluxes in and above a boreal aspen forest, *Global Change Biol.*, *2*, 219–229, 1996.

Bonan, G. B., and H. H. Shugart, Environmental factors and ecological processes in boreal forests, *Annu. Rev. Ecol. Syst.*, *20*, 1–28, 1989.

BOREAS Science Steering Committee, Charting the boreal forest's role in global change, *Eos. Trans. AGU*, *72*(4), 33–40, 1991.

Brutsaert, W., *Evaporation Into the Atmosphere*, 297 pp., D. Reidel, Norwell, Mass., 1988.

Chen, J. M., Optically based methods for measuring seasonal variation of leaf area index in boreal conifer stands, *Agric. For. Meteorol.*, *80*, 135–163, 1996.

Cosby, B. J., G. M. Hornberger, R. B. Clapp, and T. R. Ginn, A statistical exploration of the relationships of soil moisture characteristics to the physical properties of soils, *Water Resour. Res.*, *20*(6), 682–690, 1984.

Cuenca, R. H., D. E. Stangel, and S. F. Kelly, Soil water balance in a boreal forest, *J. Geophys. Res.*, this issue.

Emanuel, W. R., H. H. Shugart, and M. P. Stevenson, Climate change and the broad-scale distribution of terrestrial ecosystem complexes, *Clim. Change*, *7*, 29–43, 1985.

Evans, J. R., Photosynthesis and nitrogen relationships in leaves of C3 plants, *Oecologia*, *78*, 9–19, 1989.

Gates, D. M., *Plant-Atmosphere Relationships*, 92 pp., Chapman and Hall, New York, 1993.

Haddeland, I., and D. P. Lettenmaier, Hydrologic modeling of boreal forest ecosystems, *Water Resour. Ser. Tech. Rep.*, *143*, 123 pp., 1995.

Hanks, R. J., Soil water modelling, in *Hydrological Forecasting*, edited by M. G. Anderson and T. P. Burt, pp. 118–128, John Wiley, New York, 1985.

Hillel, D., *Fundamentals of Soil Physics*, 413 pp., Academic, San Diego, Calif., 1980.

Houghton, J. T., G. J. Jenkins, and J. J. Ephraums, *Climate Change: The IPCC Scientific Assessment*, 364 pp., Cambridge Univ. Press, New York, 1990.

Hunt, R. E., and S. W. Running, Simulated dry matter yields for aspen and spruce stands in the North American boreal forest, *Can. J. Remote Sens.*, *18*(3), 126–133, 1992.

Jarvis, P. G., and J. W. Leverenz, Productivity of temperate, deciduous and evergreen forests, in *Encyclopedia of Plant Physiology*, edited by O. L. Lange et al., vol. 12D, pp. 233–280, Springer-Verlag, New York, 1984.

Jarvis, P. G., and J. I. L. Morison, Stomatal control of transpiration and photosynthesis, in *Stomatal Physiology*, edited by P. G. Jarvis and T. A. Mansfield, pp. 247–279, Cambridge Univ. Press, New York, 1981.

Kremer, R. G., and S. W. Running, Simulating seasonal soil water balance in contrasting semi-arid vegetation communities, *Ecol. Modell.*, *84*, 151–162, 1996.

Leuning, R., Modeling stomatal behavior and photosynthesis of *Eucalyptus grandis*, *Aust. J. Plant Physiol.*, *17*, 159–175, 1990.

Manabe, S., and R. J. Stouffer, Sensitivity of a global climate model to an increase of CO_2 concentration in the atmosphere, *J. Geophys. Res.*, *85*, 5529–5554, 1980.

Monserud, R. A., N. M. Tchebakova, and R. Leemans, Global vegetation changes predicted by the modified Budyko model, *Clim. Change*, *25*, 59–83, 1993.

Neilson, R. P., and D. Marks, A global perspective of regional vegetation and hydrologic sensitivities from climatic change, *J. Vegetation Sci.*, *5*, 715–730, 1994.

Nobel, P. S., *Physicochemical and Environmental Plant Physiology*, 635 pp., Academic, San Diego, Calif., 1991.

Pastor, J., and W. M. Post, Response of northern forests to CO_2-induced climate change, *Nature*, *334*, 55–58, 1988.

Running, S. W., and J. C. Coughlan, A general model of forest ecosystem processes for regional applications, I, Hydrologic balance, canopy gas exchange, and primary production processes, *Ecol. Modell.*, *42*, 125–154, 1988.

Running, S. W., and R. E. Hunt, Generalization of a forest ecosystem process model for other biomes, BIOME-BGC, and an application for global-scale models, in *Scaling Physiologic Processes: Leaf to Globe*, edited by J. R. Ehleringer and C. B. Fields, pp. 141–158, Academic, San Diego, Calif., 1993.

Running, S. W., R. R. Nemani, and R. D. Hungerford, Extrapolation of synoptic meteorological data in mountainous terrain and its use for simulating forest evapotranspiration and photosynthesis, *Can. J. For. Res.*, *17*, 472–483, 1987.

Saxton, K.E., W. J. Rawls, J. S. Romberger, and R. I. Papendick, Estimating generalized soil-water characteristics from texture, *Soil Sci. Soc. Am. J.*, *50*, 1031–1036, 1986.

Schulze, E. D., F. M. Kelliher, C. Korner, J. Lloyd, and R. Leuning, Relationships between maximum stomatal conductance, ecosystem surface conductance, carbon assimilation and plant nitrogen nutrition: A global exercise, *Annu. Rev. Ecol. Syst.*, *25*, 629–660, 1994.

Sellers, P., et al., The Boreal Ecosystem-Atmosphere Study (BOREAS): An Overview and Early Results from the 1994 field year, *Bull. Am. Meteorol. Soc.*, *76*(9), 1549–1577, 1995.

Vowinckel, T. W., C. Oechel, and W. G. Boll, The effect of climate on the photosynthesis of *Picea mariana* at the subarctic tree line, 1, Field measurements, *Can. J. Bot.*, *53*, 604–620, 1975.

Waring, R. H., and J. F. Franklin, The evergreen coniferous forests of the Pacific Northwest, *Science*, *204*, 1380–1386, 1979.

Waring, R. H., and W. H. Schlesinger, *Forest Ecosystems Concepts and Management*, 340 pp., Academic, San Diego, Calif., 1985.

J. S. Kimball, S. W. Running, and M. A. White, NTSG School of Forestry, University of Montana, Missoula, MT 59812. (e-mail: johnk@ntsg.umt.edu)

(Received February 5, 1997; revised April 4, 1997;
accepted June 9, 1997.)